



Research paper

In situ embolism induction reveals vessel refilling in a natural aspen stand

David M. Love^{1,2} and John S. Sperry¹

¹Department of Biology, University of Utah, 257 S 1400E, Salt Lake City, UT 84112, USA; ²Corresponding author (david.m.love@utah.edu)

Received August 24, 2017; accepted January 18, 2018; published online March 2, 2018; handling Editor Frederick Meinzer

Little is known about the ability of trees to recover hydraulic conductance (k) within a growing season by regrowth or refilling of embolized conduits. Recovery of k lost to drought or other causes would prevent chronic reductions in gas exchange and productivity. To test recovery ability we conducted a 2-year experiment (2014–15) on a cohort of aspen ramets (*Populus tremuloides*, Michx.). Whole-tree k was measured from mid-June through September from sapflow (Q) and pre-dawn and mid-day xylem pressure. We induced embolism in the treatment group with high air pressure delivered by a split pressure chamber sealed around the main trunk. Successful treatments reduced k and Q by 50% or more without causing rapid desiccation. The majority of trees recovered following treatment, rising to control levels of k and Q between 12 and 17 days. Failure to recover was correlated with drier climate conditions. The growing-season recovery of k was attributed to refilling of embolized vessels, based on the absence of diameter growth. Pre-dawn xylem pressures during recovery were similar to the threshold needed to passively collapse emboli. Successful recovery during the 2-year study was consistent with no reduction in cumulative Q or canopy area in treatment vs controls. However, non-recovering trees in 2014 exhibited lower basal area growth at the start of the 2015 growing season, suggesting a linkage between recovery ability and productivity. This study provides evidence for the potential of trees to recover xylem function by refilling during the growing season.

Keywords: aspen, bubble dissolution, embolism, hydraulic stress, xylem refilling.

Introduction

Global climate change is slated to subject the world's forests to unprecedented drought stress, increasing the mortality risk of trees. Over the past century tree mortality subsequent to drought events has been on the rise, with major forest diebacks noted on every wooded continent (Allen et al. 2010). Recent work has shown that chronic hydraulic stress, induced by embolism in the tree xylem, is the most consistent indicator of ultimate tree mortality risk (Sperry and Love 2015, Adams et al. 2017). For this reason, being able to predict tree hydraulic status from climate has been identified as a major goal for understanding the impact of future drought on forest health and productivity (Anderegg et al. 2012a, 2012b, 2016, Choat et al. 2012, Powell et al. 2013, Sperry et al. 2017).

One of the major uncertainties in moving from climate to the function of tree xylem is whether or not the xylem can recover embolized transport capacity during the growing season, either

by the growth of new xylem tissue or the refilling of embolized conduits. Drought-induced cavitation can result in a legacy effect on subsequent growth (recorded in tree ring width), though this response is not always observed, even in trees subjected to severe drought stress (Anderegg et al. 2015, Cailleret et al. 2017). Data on growing season recovery by growth are scarce, likely because low xylem pressures during drought stress impose a physical limit to cell expansion, which relies on the generation of turgor pressure (Nonami and Boyer 1990).

Research has shown that predictable refilling occurs for some tree species seasonally by osmotically generated positive pressure (Hacke and Sauter 1996). Studies of potted plants have shown that there can be a variable refilling response following rewatering after drought stress (Lo Gullo et al. 2003, Brodersen et al. 2010, Secchi and Zwieniecki 2012, Ogasa et al. 2013); however, fewer studies have focused on the recovery response of naturally

growing trees (Bucci et al. 2003, Melcher and Zwieniecki 2013). Additionally, the accuracy of previous studies relying on excised branches has come into question due to a potential measurement artifact (Wheeler et al. 2013, Ogasa et al. 2016), though this artifact does not seem to affect all species and precautions taken during the harvesting process can reduce the risk of confounding the measurements (Venturas et al. 2015). Data taken from intact plants in the field could help us obtain a clearer picture of how xylem refilling impacts tree hydraulic function.

To study the response of intact trees to reductions in hydraulic conductance caused by embolism we artificially induced embolism in the trunks of naturally growing trees. We chose aspen (*Populus tremuloides* Michx.) because it is a widespread, ecologically important species in North America, and has previously been shown to be sensitive to dieback associated with drought-induced embolism (Anderegg et al. 2012a, 2012b). In our experiment we induced embolism using a split pressure chamber in the main trunk of young aspen ramets (above ground stems) below the canopy. Tree sapflow and hydraulic conductance were subsequently monitored for the magnitude of post-treatment recovery. Specifically we aimed to assess: (i) the extent of recovery of hydraulic conductance during the growing season; (ii) whether observed recovery could be attributed to growth or refilling; and (iii) the impact of reduced growing-season hydraulic conductance on growth, water use and survival.

Materials and methods

Study location

The study site is located in the Red Butte Canyon Research Natural Area (40.806112 N, 111.765454 W). This is a mid-montane habitat (1950 m elevation) and is in the transition zone between lower elevation mixed oak–maple forest and mid-montane aspen–fir forest. The monitoring period was from June to September in 2014 and 2015. Trees were located ~10–30 m from a perennial stream (Knowlton's Fork Creek) on a south-east facing slope. Relativity humidity and air temperature were measured on site every 10 min (HMP-50-L; Campbell Scientific, Logan, UT, USA). Precipitation data were obtained from a weather station located within the same drainage (iUTAH GAMUT Working Group (2017), iUTAH GAMUT Network Raw Data at Knowlton Fork Climate (RB_KF_C), HydroShare, <http://www.hydroshare.org/resource/74dc57ed714e4cd3882edc16d50e197a>). Twenty young aspen ramets were chosen in 2014 from a stand of similar sized saplings divided by a small game trail. Ramets ranged from ~1.5 to 3 m in height and 2.1 to 3.4 cm in basal diameter.

Measurement of whole-tree transpiration and hydraulic conductance

Heat balance sensors were used to measure whole-tree sapflow (Q), which is equivalent to whole-tree transpiration rate (E) under steady-state conditions likely to prevail for the small

saplings measured. Sensors were constructed according to the methods of Baker and Van Bavel (1987). In this method the dissipation of power emitted by a flexible heater wrapped around the stem (W_{in}) is accounted for by a series of thermocouples. Power can be transmitted radially through the sensor to the atmosphere (W_r), axially through the stem (W_{ax}) or convectively through the xylem sap (W_o). Power may also be stored in the stem tissue (W_s). Convective heat loss by sapflow was solved from the heat balance equation in the following way:

$$W_o = W_{in} - W_r - W_{ax} - W_s \quad (1)$$

To account for W_r the thermal conductance of the sensor (k_{sh}) must be known. This value varies based on the sensor installation and is calculated when sapflow is assumed to be equal to zero. We calculated k_{sh} nightly between 0:00 and 5:00 h for each sensor when the radial heat gradient was at its peak. Sensors were constructed using flexible kapton heaters (Heater Designs Inc., Bloomington, CA, USA) with an approximate resistance of 60 Ω . Sensor power was supplied from 12 V deep cycle batteries using adjustable voltage regulators to keep sensor power output at 3.375 W (Dimension Engineering, Akron, OH, USA). Sensor output was recorded using a CR-7 datalogger (Campbell Scientific). Sensors were installed on the main trunk below lateral branches early in June and removed in late September of the same year. The sensors were placed >0.5 m above the soil surface; in treatment trees the split chamber was installed above the sapflow sensor. All sensors were insulated using 2.5-cm thick closed cell foam and additionally wrapped in bubble-foil type insulation. Sensor accuracy was tested in the laboratory by comparing sensor output to flow rates directly measured with an analytical balance (BP 211D, Sartorius Corporation, Bohemia, NY, USA). Sensor flow was not statistically different (Student's t -test, $P > 0.4$) from balance measured flow within the range observed in the field (0–0.035 $g\ s^{-1}$).

To estimate whole-tree hydraulic conductance (k_t) from whole-tree sapflow we used the following relationship:

$$k_t = Q_{md} / (P_{pd} - P_{md}), \quad (2)$$

where Q_{md} is the average sapflow rate between 12:00 and 14:00 h and P_{pd} and P_{md} are pre-dawn and mid-day xylem pressure, respectively. The difference between P_{pd} and P_{md} is equivalent to the soil to canopy pressure drop (ΔP) at mid-day during peak sapflow (measurements were made at similar canopy heights (~2 m), canceling the gravitational pressure drop). Equation (2) assumes steady-state conditions with no capacitive exchange between the transpiration stream and plant storage. For this reason, we limited k estimation to mid-day hours on clear days with a vapor pressure deficit (D) above 1.5 kPa. These conditions saturated and stabilized Q_{md} and P_{md} , which together with the small sapling size would promote steady-state

flow. Xylem pressures were measured on a weekly or bi-weekly basis on leaves using a Scholander type pressure bomb (PMS, Corvallis, OR, USA), except for before and after the split pressure chamber treatment when additional measurements were made. The near constant mid-day and pre-dawn xylem pressures between treatment groups and seasons (see Results) would tend to make any deviation from steady-state relatively consistent across the study period. To quantify the impact of the split chamber treatments on pre-treatment hydraulic conductance and facilitate comparisons between trees, k_t and Q_{md} were normalized relative to each tree's maximum seasonal value (k_{max} , Q_{max}):

$$k_r = (k_t/k_{max}); \quad (3)$$

$$Q_r = Q_{md}/Q_{max}. \quad (4)$$

Split chamber treatments

Out of the cohort of 20 aspen saplings, five trees were designated as controls and 15 as treatments. In order to induce embolism in the treatment trees a split pressure chamber was installed around the base of the main trunk and pressurized using nitrogen gas (methods similar to those employed by Hubbard et al. (2001), though bark was left intact). The chamber is cylindrical, with a diameter of 3.2 cm and a height of 11 cm. The chamber is capped at the top and bottom by #11 rubber stoppers, and the side seams are chamfered to hold a split o-ring type gasket. The seams and rubber stoppers were sealed using silicone caulking. The split chamber induces embolism via air-seeding, where the driving force for meniscal failure in the pit membranes is quantified by the pressure difference between gas filled conduits (P_{gas} , usually equal to atmospheric pressure, conventionally set to 0), and water filled conduits which are usually negative (P_{sap}).

$$\Delta P = P_{gas} - P_{sap}. \quad (5)$$

In the split chamber the pressure of gas filled conduits is raised far above atmospheric pressure to increase ΔP and force air bubbles across pit membranes, which 'seed' the phase change of metastable xylem sap, forming emboli in affected conduits. The split chamber treatments targeted a level of trunk embolism between 60% and 80% loss of conductance, requiring a ΔP of 3 MPa based on a published vulnerability curve for aspen from a nearby watershed (Sperry and Sullivan 1992). This ΔP was sustained for 30 min. To measure P_{sap} , several small branches were bagged on each treatment tree at pre-dawn the morning before the split chamber treatment. Bagging promoted the equilibration of twig and stem xylem pressures. Before pressurization the P_{sap} was measured on a bagged twig using the Scholander pressure chamber. The P_{sap} was again measured after 15 min and then again at the end of the

treatment. If xylem pressure changed significantly after the first 15 min the chamber pressure was adjusted as required by Eq. (5) to maintain the target ΔP . The split chamber treatments were applied between the hours of 9:00 and 19:00 h in 2014 and only after 20:00 h in 2015. The switch to evening treatments was done to minimize the accidental induction of rapid canopy desiccation as observed in a subset of treated trees in 2014 (see Results).

The initial split chamber treatment occurred over the interval between 4 and 10 July 2014 following the establishment of a pre-treatment baseline of sapflow and hydraulic conductance, and after the bulk of the season's basal diameter growth was expected. Immediate treatment impact was assessed from the mean difference in k_r and Q_r between control and treatment trees on the first day of record after treatment (i.e., 'flow-saturating' days meeting the $D > 1.5$ plus clear sky conditions). Subsequent recovery was assessed by a significant increase in mean Q_r and k_r relative to the immediate post-treatment mean using a Student's *t*-test. Trees showing recovery were re-treated using the same protocol to determine if the recovery was reproducible. As further described under Results, these additional treatments occurred on 8–9 August 2014 and 4–10 July 2015.

To measure the distribution and extent of embolism induced by the split chamber method, three trees in the study area were treated with the standard treatment protocol and subsequently cut underwater along with three adjacent control trees and brought to the laboratory (<25 min away). The trees were divided into unbranched 10 cm segments from the main trunk, including segments above, below and at the site of the pressure chamber installation. Segments of this length are likely to contain <1% open vessels based on measurements of vessel length from an adjacent stand (Sperry et al. 1991). These segments were cut underwater, shaved using fresh razor blades, and measured for native and maximum hydraulic conductivity using the methods described in Torres-Ruiz et al. (2012).

Stem diameter and canopy leaf area

The influence of treatments on tree growth and vigor were assessed from trunk diameter growth and canopy leaf area. Stem diameter was measured at two locations using manual calipers to assess growth, including just above the root crown (basal diameter) and within 5 cm of sensor installation (either above or below). At each location the diameter was measured at two points along the circumference of the trunk to obtain an average diameter. The position for the caliper jaws were marked on the bark using a permanent marker so that average diameter was always determined from the same measurements. Diameter was measured at the beginning and end of the growing season. In the same manner stem diameter at the site of the pressure chamber was also measured to look for anomalous post-treatment recovery by xylem growth and at the location of the heat balance sensor as required to solve the heat balance equations.

Canopy leaf area was estimated from whole-tree leaf number, average leaf length per tree, and the leaf length to area relationship derived for the study site. Leaf number was assessed near the time of sensor installation (mid-June) and again in August of 2014. In 2015 additional measurements were made in late August and September. In 2015, study trees became infected with leaf spot fungus (*Marssonina brunnea*) and leaf drop occurred earlier and more extensively than in 2014. To determine average leaf length per individual tree, leaf lengths were measured for all the leaves on two lateral branches as well as the leader in early 2014 using dial calipers with 0.1 mm dial ticks. To obtain the leaf length to area relationship entire branches were sampled from additional trees within the same stand. These branches included a mix of leaders and lateral branches. Leaf length was measured using calipers and area was measured using a leaf area meter for 217 individual leaves (LI-3100, LICOR Biosciences, Lincoln, NE, USA). A linear regression of leaf length to area was fit to those data and used to provide estimates of canopy leaf area from the leaf number and average leaf length data.

Results

Seasonal dynamics of xylem pressure

Pre-dawn xylem pressures remained high in both years and showed no difference between controls and treatments (Figure 1; Student's *t*-test, $P > 0.5$), indicating a favorable root water supply as was expected for the riparian study site. In 2014 pre-dawn pressures were nearly constant, averaging -0.1 ± 0.01 MPa (mean \pm SE). In 2015 pre-dawn pressures dropped gradually

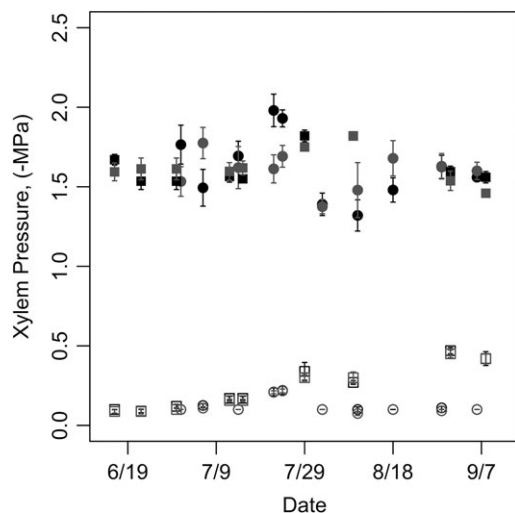


Figure 1. Mean mid-day (closed symbols) and pre-dawn (open symbols) xylem pressures \pm SE from treatment (gray) and control (black) in both years of the study (circles 2014, squares 2015). There was no significant difference between treatment groups, and growing seasons for mid-day xylem pressures and pre-dawn to mid-day pressure drop at the study location. Measured pre-dawn was slightly lower in 2015 than in 2014.

from -0.1 MPa in late June to -0.5 MPa by the end of August, averaging -0.23 ± 0.08 MPa (Figure 1). Mid-day pressures did not differ between treatments and controls within a year (season 2014: -1.62 ± 0.1 MPa control, -1.59 ± 0.04 MPa treatment; season 2015: -1.63 ± 0.05 MPa control, -1.62 ± 0.04 MPa, treatment; Student's *t*-test, $P > 0.6$), or between years (season 2014 1.61 ± 0.05 , season 2015 1.62 ± 0.08 ; Student's *t*-test, $P = 0.8$). Mid-day pressure drop did not differ between the years, within the year, or within the season, averaging 1.48 ± 0.11 MPa ($P = 0.8$). The fact that xylem pressures on flow-saturating days were relatively constant throughout the growing season meant that any differences in mid-day flow rate (Q_{md}) on such days could be attributed to changes in tree hydraulic conductance (k). Changes in Q_{md} served as a more continuously measured proxy for changes in k .

Seasonal dynamics of hydraulic conductance and sapflow in control trees

In both years, the control trees reached their seasonal maxima for Q_{md} ($Q_r = 1$) and k_t ($k_r = 1$) early in the growing season and values remained relatively stable before gradually declining towards the season's end. Control Q_r by 8 September fell to 0.56 ± 0.08 in 2014, and to 0.32 ± 0.065 in 2015 (Figure 2, black lines). Control k_r at this time was 0.67 ± 0.08 in 2014, and 0.39 ± 0.06 in 2015 (Figure 2, black circles). The late-season drop in hydraulic conductance was associated with a drop in canopy leaf area (Figure 2, black triangles), as was particularly evident in 2015 when late season leaf area was assessed multiple times during the leaf-spot infection.

Response of sapflow and hydraulic conductance to split chamber treatments

Prior to being treated for the first time in 2014, the 15 tree treatment group averaged comparable k_t (per basal area) as control trees (control 0.00051 ± 0.01 g MPa $^{-1}$ mm $^{-2}$ s $^{-1}$, treatment 0.00048 ± 0.01 g MPa $^{-1}$ mm $^{-2}$ s $^{-1}$; Student's *t*-test, $P = 0.8$). The first embolism treatment occurred in early July 2014. Thirteen of the 15 treatments were successful in causing substantial reductions in tree sapflow and hydraulic conductance without triggering immediate death by desiccation. These successfully treated trees showed an abrupt decline in sapflow during the treatment and in the hours following (e.g., Figure 3a), while maintaining typical xylem pressures. On the next day of record (i.e., flow-saturating day with $D > 1.5$ kPa) these 13 surviving trees showed a mean k_r 0.35 ± 0.07 vs 0.90 ± 0.02 for controls, and a mean Q_r of 0.36 ± 0.05 relative to 0.91 ± 0.08 in controls; both significant reductions (Student's *t*-test, $P < 0.01$). The two unsuccessful treatments caused rapid desiccation and death. Unlike the surviving trees, the dying trees showed no reduction in sapflow during and after treatment. Instead, sapflow remained near normal during and after the treatment before abruptly plummeting to zero within a few hours

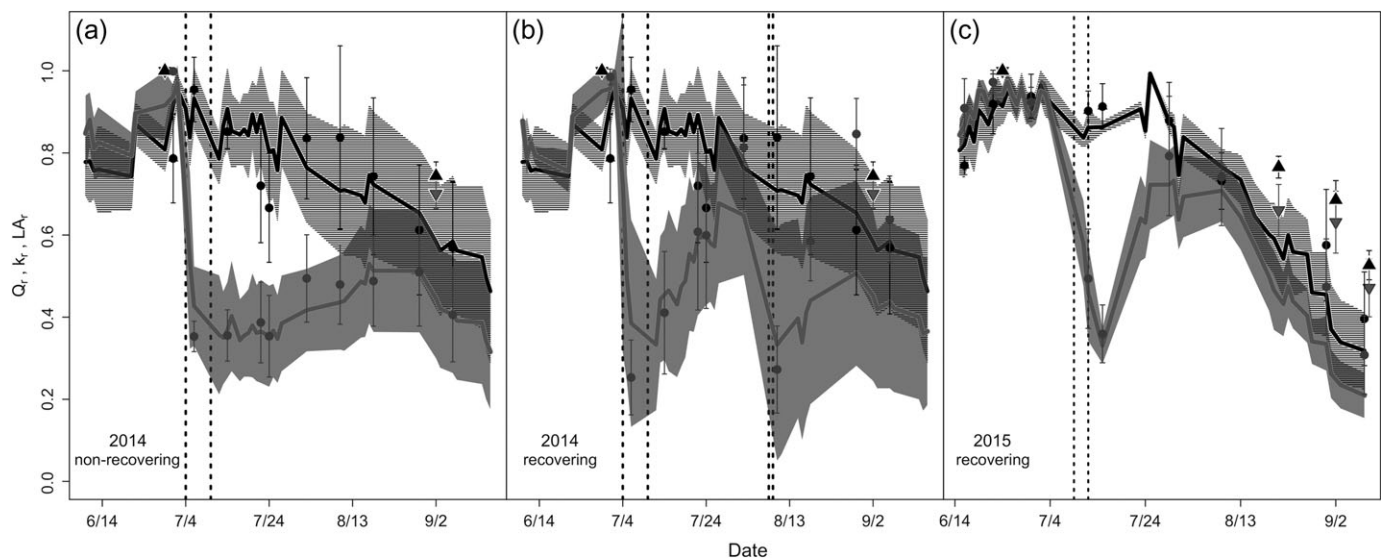


Figure 2. Time course of hydraulic conductance (k_t), sapflow rate (Q_r) and canopy leaf area (LA_r), relative to seasonal maxima for 2014 and 2015. Control (black) and treatment (gray) Q_r is plotted as a line with a hatched (control) or gray shaded upper and lower 95% CIs. Control and treatment k_t are plotted as filled black and gray circles, respectively, with error bars representing the 95% CI. Black and gray triangles and associated bars represent the mean changes in relative canopy area (LA_r) \pm SE for control and treatment trees respectively. Vertical dashed lines denote the interval over which split chamber treatments occurred. (a) 2014 non-recovering trees that were treated once ($n = 6$ successful treatments) and showed no significant increase from post-treatment k_t and Q_r . (b) 2014 recovering trees that showed significant increase from post-treatment k_t and Q_r ($n = 7$), and recovered again from a subsequent treatment ($n = 3$ successful treatments). (c) All successfully treated trees ($n = 8$) recovered in 2015 from a single treatment.

(e.g., Figure 3b). These dying trees exhibited extremely negative xylem pressures at pre-dawn following the treatment (-1.5 to -4 MPa vs above -0.5 in controls) and the canopy was completely desiccated by the afternoon.

Six of the 13 successfully treated trees showed no significant recovery in k_t or Q_r relative to the immediate post-treatment value during the 50 days remaining in the 2014 growing season (Student's t -test, $P > 0.07$, Figure 2a). The overlap with control k_t and Q_r by season's end was largely due to the decline in controls rather than any statistically significant recovery of transport capacity in treatments.

Seven of the 13 surviving trees did show an appreciable increase in k_t and Q_r following treatment. The increase in k_t was significant within 12 days, rising from 0.34 ± 0.07 immediately following treatment, to 0.60 ± 0.09 (Student's t -test, $P = 0.04$). The Q_r also increased significantly within 17 days, rising from 0.33 ± 0.07 to 0.62 ± 0.08 (Student's t -test, $P = 0.03$). Both k_t and Q_r rose to control values (Figure 2b) within 12 days of treatment.

To test for the reproducibility of recovery, this 'recovering' group underwent an additional split chamber treatment on 8 and 9 August 2014. Unfortunately, four of the seven treatments were unsuccessful and resulted in zero sapflow and canopy desiccation the day after treatment. The three successful treatments caused k_t and Q_r to drop well below control values (k_t , 0.33 ± 0.11 vs 0.83 ± 0.11 for controls; Q_r , 0.25 ± 0.11 vs 0.70 ± 0.07 for controls; Student's t -test, $P < 0.01$) without killing the trees. Trees once again showed a strong recovery response, rising to control levels in the following weeks (Figure 2b).

There was no evidence of any carry-over effect of the 2014 treatments into 2015. There was no difference in absolute hydraulic conductance (k_t , per basal area) between the treatment and control groups at the beginning of the 2015 season (control 0.00030 ± 0.01 g MPa $^{-1}$ mm $^{-2}$ s $^{-1}$, treatment 0.00028 ± 0.01 g MPa $^{-1}$ mm $^{-2}$ s $^{-1}$; Student's t -test, $P = 0.6$). The overall mean k_t was lower at the start of 2015 vs 2014, though this trend was not significant (Student's t -test, $P = 0.06$). Lower hydraulic conductance in 2015 was likely a symptom of the leaf spot infection in 2015.

Following the period of pre-treatment monitoring, the split chamber was applied to the nine remaining treatment trees in early July 2015. The 2015 treatments were applied after sunset (21:15–21:45 h) to minimize the induction of rapid death, and only one tree died from canopy desiccation. The treatment impact was similar in magnitude to 2014 (mean k_t , 0.42 ± 0.04 vs 0.91 ± 0.03 in controls; mean Q_r , 0.32 ± 0.05 vs 0.86 ± 0.4 in controls, Student's t -test, $P < 0.01$). All surviving treated trees showed a significant increase in k_t and Q_r in the month following the treatment. The first significant increase in Q_r was recorded 11 days following treatment application, rising from 0.32 ± 0.05 to 0.64 ± 0.03 (Student's t -test, $P < 0.01$). Significant increases in k_t were noted on the first post-treatment measurement day, 17 days following treatment (Figure 3). This day also corresponded with the first day that k_t and Q_r reached control values. At the end of the 2015 season, the treatment and control Q_r were not significantly different (control 0.32 ± 0.10 , treatment 0.21 ± 0.08 ; Student's t -test, $P = 0.27$).

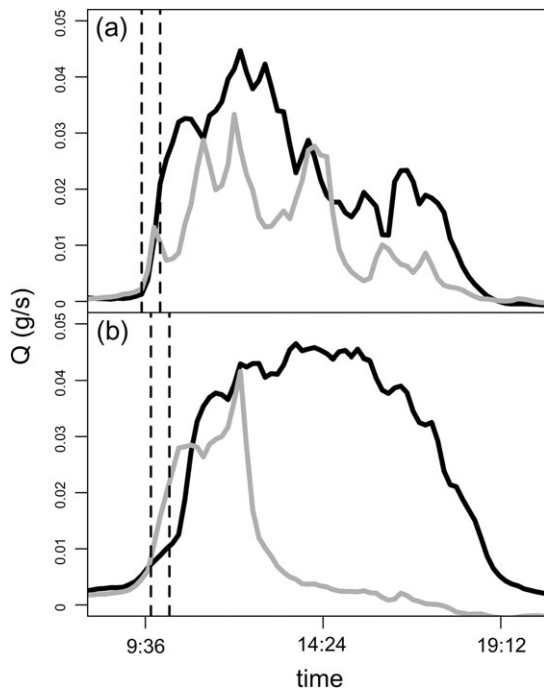


Figure 3. Immediate impact of split chamber treatments on whole-tree sapflow. All traces are from flow saturating days ($D > 1.5$ kPa). Black lines are from the day before the split chamber treatment, exemplifying the 'normal' dynamics of daytime sapflow. Gray lines are traces from the treatment day. Vertical dashed lines indicate the time interval over which the split chamber was installed. (a) Sapflow traces from a successfully treated tree that survived the embolism induction. Even before the end of the treatment, the tree had reversed the typical morning increase in Q , and maintained sub-normal flow rates for the remainder of the day. Xylem pressures remained normal. (b) Sapflow trace from an unsuccessful treatment that triggered rapid desiccation and death. During the treatment, Q continued to show a marked rise, and post-treatment Q initially remained near normal before spiking and plummeting to near zero. Post-treatment xylem pressures were far below the pre-treatment value and the leaves were desiccated by dawn of the next day.

Magnitude and extent of embolism caused by the split chamber treatment

The embolism induced by the split chamber method was highly localized to the site of chamber installation, with no detectable axial spread up and down the trunk. Segments within 15 cm above and below the site of the chamber installation showed similar values of native hydraulic conductivity per stem area compared to equivalent sections of control trees (2.08 ± 0.055 g mm⁻¹ MPa⁻¹ control, 1.88 ± 0.012 g mm⁻¹ MPa⁻¹ treatment). Segments taken from the site of the split chamber showed very low levels of hydraulic conductivity (0.0232 ± 0.0032 g mm⁻¹ MPa⁻¹), averaging a 98.8% loss of hydraulic conductance (PLC) relative to the mean value (1.96 ± 0.079 g mm⁻¹ MPa⁻¹) for other measured segments. This pattern of embolism induction is expected to have minimal impacts on whole-tree hydraulic conductance until very high values of trunk segment PLC (see Discussion).

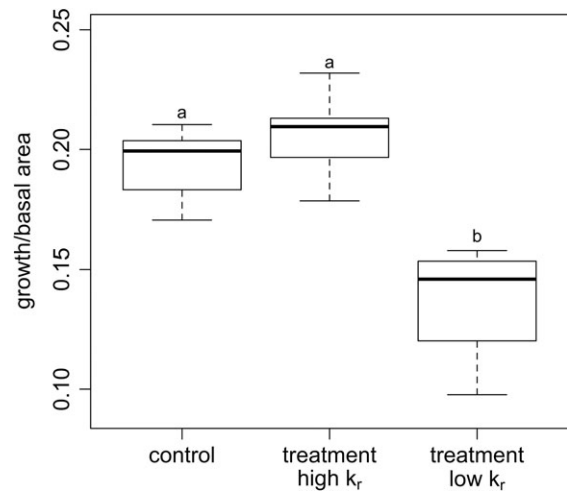


Figure 4. Basal area growth normalized per initial basal area for the period between the end of the 2014 field season and the start of the 2015 growing season. Basal area was computed as the area of an equivalent circle based on the average of two diameter measurements. Letters denote statistical difference according to a Tukey HSD test ($P < 0.01$). Treatment 'low k_r ' trees experienced mean seasonal $k_r < 0.5$ during the 2014 growing season, and showed lower growth than treatment 'high k_r ' trees (mean $k_r > 0.5$) or the control group.

Treatment impacts on cumulative water use and growth

To assess the treatment impact on growing season water use, the cumulative Q (normalized per trunk basal area) was summed over the monitoring period in 2014 and 2015 between the hours of 9:00 and 21:00 h (including all days before and after treatment, and regardless of D). Treatment trees exhibited lower cumulative Q /basal area, though this trend was not significant (184 kg m⁻² treatment, 284 kg m⁻² control, Student's t -test, $P = 0.26$). The impact of the treatment was mitigated by the recovery seen in most trees, especially in 2015. We observed no significant difference in stem diameter growth normalized per basal area between the treatment and control groups, the timing of seasonal leaf drop and the recovery of canopy area between seasons (Student's t -test, $P > 0.2$).

However, significant differences in basal area growth were observed for a subset of four treatment trees between the 2014 and 2015 growing seasons. These trees were all part of the non-recovering group in 2014 (Figure 2a), and additionally had mean seasonal values of k_r and $Q_r < 0.5$ (treatment-low k_r , Figure 4). Mean seasonal values of k_r and Q_r were above 0.6 in other treatments (treatment-high k_r , Figure 4), and means for controls were > 0.75 . All three groups differed significantly in terms of mean k_r and Q_r (Tukey HSD, $P < 0.01$), however the high k_r treatment group and control were indistinguishable in terms of basal area growth (Tukey HSD, control vs high k_r treatment $P = 0.6$, control vs low k_r treatment $P < 0.01$, high k_r treatment vs low k_r treatment $P < 0.01$).

Climatic variables associated with recovery

The more consistent recovery of k_r and Q_r in the 2015 growing season was associated with both higher precipitation, and lower mid-day D in the interval immediately preceding and following the split chamber treatment application (1 July to 7 August). This interval corresponds to three days before the first round of split chamber treatments in 2014, and prior to the application of the second treatment in 2014. Cumulative precipitation over this interval was 5.1 cm in 2014, and 7.5 cm in 2015. Mid-day D (averaged from 11:00 to 15:00 h, during the daily peak in sap-flow) was 1.9 ± 0.13 kPa in 2014, and 1.3 ± 0.1 kPa in 2015.

Discussion

This study provides evidence for the ability of aspen to recover hydraulic conductance within a growing season. Because the post-treatment rise in hydraulic conductance occurred in the absence of measurable basal diameter growth we attribute the recovery to refilling of embolized xylem conduits. As a result of recovery, our treatments had limited impacts on whole-season water use and treated trees showed minimal legacy effects. The exception was low basal area growth in four non-recovering treatment trees in 2014 with the lowest post-treatment hydraulic conductance (Figure 4). All trees, control and treatment alike, showed a rebound in tree hydraulic conductance in the 'off season' when measurements were not made. Such recovery was likely associated with the growth of new canopy, and possibly post-snowmelt refilling. Other than the accidental deaths from rapid desiccation, successful split chamber treatments were not associated with mortality pursuant to chronically low gas exchange because of the transient nature of the treatment impact.

Reversal of embolism by xylem refilling has become a much investigated, and also very controversial topic in plant hydraulics (Venturas et al. 2017). Of particular interest is whether xylem emboli are able to refill while the bulk xylem pressure is below the limits that would be expected for the passive dissolution of the trapped gas bubble. Refilling that occurs at a bulk xylem pressure below these limits would require the independent pressurization of the bubble by an as yet unknown 'novel' mechanism, perhaps relying on pressurization via phloem and xylem parenchyma (Salteo et al. 2009, Nardini et al. 2011, Christman et al. 2012, Secchi et al. 2017). Xylem pressure thresholds for bubble dissolution (P_{refill}) range from a lower pressure limit for water vapor filled emboli, to an upper pressure limit for air filled emboli (Yang and Tyree 1992)

$$P_{\text{refill}} > B_{\text{dissolve}} - 2T/r. \quad (7)$$

The B_{dissolve} is the gas bubble pressure that must be exceeded for the embolus to dissolve, T is the surface tension of water and r is the radius of the conduit and as a result the radius of curvature of the embolus. B_{dissolve} equals the saturated vapor pressure of water for a vapor embolus, or atmospheric pressure

(79.9 kPa at the site) for an air embolus. To calculate P_{refill} , we used the mean night time temperature for both years (11.12 °C), yielding 0.074 nm^{-1} for T , and a saturated water vapor pressure of 1.42 kPa. Values for aspen vessel radius were taken from Schreiber et al. (2011), using a mean vessel radius of 12.5 μm . The expected P_{refill} (relative to $P_{\text{atm}} = 0$) was between ~ -0.1 MPa for vapor filled emboli and -0.04 MPa for air filled emboli. Because of the timing over which recovery occurred (periods over 1 week) and the nature of embolism induction using our method where pressurized air is forced into conduits, the emboli were most likely air filled, favoring the use of the upper limit of -0.04 MPa (Wang et al. 2015).

Based on our xylem pressure data it is difficult to determine whether the refilling observed in our case was passively driven by bulk xylem pressure, or required active pressurizing of the emboli. Pre-dawn bulk xylem pressures were too close to P_{refill} (-0.04 MPa for air emboli), and too infrequently measured, to decisively refute a passive refilling process. In the interval following the treatment when refilling was observed mean pre-dawn pressure was -0.13 ± 0.02 MPa in 2014, and -0.24 ± 0.08 MPa in 2015. Though these mean pre-dawn pressures were below the threshold needed for dissolution of air filled emboli in both years, pre-dawn pressures were assessed weekly or bi-weekly, and targeted days when flow saturating conditions were expected at mid-day. Days where pre-dawn pressures were high enough to promote refilling could have easily been missed by our sampling scheme, particularly in 2015 when the post-treatment period had more frequent and larger rain events.

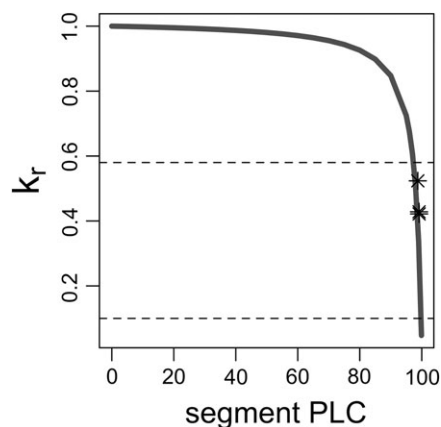


Figure 5. Theoretical relationship between embolism within the treated stem segment (segment PLC, percent loss of hydraulic conductance) and whole-plant hydraulic conductance relative to maximum (k_r). The relationship assumed all embolism was confined to the treated stem segments as was observed, and that untreated segments comprised 2% of the average whole-plant resistance as estimated from measurements. Very high segment PLC is required to reduce whole-tree k_r . Asterisks show the estimated effect on k_r for the PLC measured on three treated segments. Horizontal dotted lines denote the approximate k_r range for successful treatments over both seasons. Only a small amount of refilling in the heavily embolized treatment segments would result in large overall gains in whole-tree conductance.

The axially constricted nature of the gas blockage suggests that very little local refilling would be necessary to cause a significant recovery in whole-plant hydraulic conductance. The split chamber treatment produced a threshold type effect on whole-plant hydraulic conductance where the local segment embolism needs to become extremely high before effects on whole-plant water transport capacity (k) begin to manifest. This threshold response was modeled (in Figure 5) by assuming that the treated trunk segment and the rest of the plant act as hydraulic resistors (hydraulic resistance, $r = 1/k$) in series.

$$r_{\text{plant}} = r_{\text{segment}} + r_{\text{remainder}} \quad (8)$$

For untreated plants, r_{plant} was determined from the mean values of maximum tree hydraulic conductance per basal area (i.e., control and pre-treatment) obtained in 2014 and 2015 (k_{plant} , $0.0004 \text{ g MPa}^{-1} \text{ mm}^{-2} \text{ s}^{-1}$). The untreated r_{segment} was estimated from the mean hydraulic conductance (conductivity divided by segment length) of excised trunk segments from non-injected trees measured in the laboratory (k_{segment} , $0.02 \text{ g MPa}^{-1} \text{ mm}^{-2} \text{ s}^{-1}$). For untreated trees, a trunk segment equivalent to those treated in the field would account for about 2% of the whole-plant resistance before treatment. Only when this segment is over 98% embolized do we see plant k_r falling within the range we observed following treatment with the split chamber. This is also consistent with the three treated segments that were measured using the conductivity apparatus, which on average had 98.8% lower hydraulic conductance than native values recorded for other stem segments. As a result, a small number of refilled emboli (~1% of the induced embolism) could induce a near total recovery at the whole-plant scale. The fact that we observed incomplete or absent post-treatment recovery in some trees indicates that the mechanism leading to recovery was prone to failure, even at the modestly negative xylem pressures we measured at our study site. This runs counter to what would be predicted for an active response that has evolved to insure rapid and consistent post-drought recovery.

For this reason, we caution using the results of our study to suggest that aspen has the ability to rapidly recover hydraulic conductance following drought. Treatments using the split pressure chamber are highly artificial and do not simulate the pattern of whole-plant embolism induced by natural drought, which would require more pervasive refilling to result in recovery. In fact, field studies have documented prolonged post-drought mortality events in this species that co-occur with a failure to effectively recover transport capacity (Anderegg et al. 2013). If the recovery we observed was passive, as we suspect, it is highly unlikely that drought-stressed trees would experience post-drought xylem pressures high enough to promote extensive refilling throughout the tree.

Our results add to the growing body of evidence that successful stomatal control in plants is tightly coupled to hydraulic

conductance of the network (Wolf et al. 2016, Sperry et al. 2017). Successfully treated plants responded by lowering sapflow (necessarily via stomatal closure) while maintaining the same mid-day leaf xylem pressure. This stomatal response was elicited in the complete absence of any drought, indicating a stomatal closure mechanism that operates independently of soil or root water status. Most likely the closure signal is generated somewhere in the leaf tissue, where the stomata are being regulated via rapid negative feedback with temporarily falling leaf water potential. Such feedback would result in leaf water potential oscillating around a physiological set point, resulting in a near homeostasis in bulk tissue water potential (analogous to thermostatic regulation of room temperature). The short-term response to the split chamber treatment reported in Figure 3a for a surviving tree is consistent with this hypothesis. This tree exhibited a rapid reduction in whole-plant sapflow in response to the split chamber treatment and showed no detectable drop in leaf xylem pressure. The dying tree example in Figure 3b suggests there is a limit to how rapidly the stomata can respond. Trees that died from the treatment failed to restrict sapflow in response to the reduced hydraulic conductance, resulting in an unregulated drop in xylem pressure that desiccated the plant within 24 h. It is possible that these dying trees experienced a greater initial reduction in tree hydraulic conductance (even to near zero despite air pressure adjustment), which would require a faster stomatal response to prevent runaway xylem pressures and embolism. Notably, when we switched to evening treatments in 2015, we lost only one tree to desiccation (~11%) vs five fatalities (~24%) for the daytime treatments of 2014. Low evening sapflow rates would minimize the potential pressure drop caused by the treatment, and would require a less rapid stomatal response time.

While the split chamber method does have short comings in terms of its ability to directly simulate the effects of drought in terms of the highly artificial pattern of embolism induction, it does hold promise as an extremely sensitive assay for refilling ability in intact woody plants. While at our site high available soil moisture made it difficult to definitively detect an active refilling mechanism, experiments of this design in drier soils (i.e., where pre-dawn pressure is assuredly lower than bubble dissolution thresholds) could be used to very sensitively detect the presence of novel embolism reversal. In addition, the split chamber could be used to further study the stomatal responses to hydraulic conductance in intact plants. The ability to induce embolism on a short timescale allows for detailed study of the timescale over which stomata are able to respond to increased resistance of the flow path. This could prove insightful for investigating the stomatal behavior of lineages of woody plants that show varying responses to abscisic acid, which are already shown to respond on different timescales to changes in air vapor pressure deficit (Brodrribb and McAdam 2011).

Acknowledgments

The authors would like to thank Craig Lanning, Toshihiro Umabayashi and Allison Thompson, who helped collect field data, and Martin Venturas, Yujie Wang, Duncan Smith and Maurizio Mencuccini provided suggestions on the data analysis.

Conflict of interest

None declared.

Funding

Funding was provided for the project by NSF-IOS-1450650 and support to D.M.L. through the University of Utah.

References

- Adams HD, Zeppel MJB, Anderegg WRL et al. (2017) A multi-species synthesis of physiological mechanisms in drought-induced tree mortality. *Nat Ecol Evol* 1:1285–1291.
- Allen C, Macalady A, Chenchouni H et al. (2010) A global overview of drought and heat-induced tree mortality reveals emerging climate change risks for forests. *For Ecol Manage* 259:660–684.
- Anderegg W, Berry J, Field CB (2012a) Linking definitions, mechanisms, and modeling of drought-induced tree death. *Trends Plant Sci* 17: 693–700.
- Anderegg W, Berry J, Smith D, Sperry J, Anderegg L, Field CB (2012b) The roles of hydraulic and carbon stress in a widespread climate-induced forest die-off. *Proc Natl Acad Sci USA* 109:233–237.
- Anderegg W, Placova L, Anderegg L, Hacke U, Berry J, Field CB (2013) Drought's legacy: hydraulic deterioration underlies widespread aspen die-off and portends increased future vulnerability. *Glob Chang Biol* 19:1188–1196.
- Anderegg W, Schwalm C, Biondi F et al. (2015) Pervasive drought legacies in forest ecosystems and their implications for carbon cycle models. *Science* 349:528–532.
- Anderegg W, Klein T, Bartlett M, Sack L, Pellegrini B, Choat B, Jansen S (2016) Meta-analysis reveals that hydraulic traits explain cross-species patterns of drought-induced tree mortality across the globe. *Proc Natl Acad Sci USA* 113:5024–5029.
- Baker JM, Van Bavel CHM (1987) Measurement of mass flow of water in the stems of herbaceous plants. *Plant Cell Environ* 10:777–782.
- Brodersen C, McElrone A, Choat B, Matthews M, Shackel KA (2010) The dynamics of embolism repair in xylem: in vivo visualizations using high-resolution computed tomography. *Plant Physiol* 154:1088–1095.
- Brodribb T, McAdam SAM (2011) Passive origins of stomatal control in vascular plants. *Science* 331:582–585.
- Bucci S, Scholz F, Goldstein G, Meinzer F, Sternberg LDSL (2003) Dynamic changes in hydraulic conductivity in petioles of two savanna species: factors and mechanisms contributing to the refilling of embolized vessels. *Plant Cell Environ* 26:1633–1645.
- Cailleret M, Jansen S, Robert EMR et al. (2017) A synthesis of radial growth patterns preceding tree mortality. *Glob Chang Biol* 23: 1675–1690.
- Choat B, Jansen S, Brodribb T et al. (2012) Global convergence in the vulnerability of forests to drought. *Nature* 491:752–755.
- Christman M, Sperry J, Smith DD (2012) Rare pits, large vessels, and extreme vulnerability to cavitation in a ring-porous tree species. *New Phytol* 193:713–720.
- Hacke U, Sauter JJ (1996) Xylem dysfunction during winter and recovery of hydraulic conductivity in diffuse-porous and ring-porous trees. *Oecologia* 105:435–439.
- Hubbard R, Stiller V, Ryan M, Sperry JS (2001) Stomatal conductance and photosynthesis vary linearly with plant hydraulic conductance in ponderosa pine. *Plant Cell Environ* 24:113–121.
- Lo Gullo MA, Nardini A, Trifilò P, Salleo S (2003) Changes in leaf hydraulics and stomatal conductance following drought stress and irrigation in *Ceratonia siliqua* (Carob tree). *Physiol Plant* 117: 186–194.
- Melcher P, Zwieniecki M (2013) Functional analysis of embolism induced by air injection in *Acer rubrum* and *Salix nigra*. *Front Plant Sci* 4:368.
- Nardini A, LoGullo M, Salleo S (2011) Refilling embolized xylem conduits: is it a matter of phloem unloading? *Plant Sci* 180: 604–611.
- Nonami H, Boyer JS (1990) Primary events regulating stem growth at low water potentials. *Plant Physiol* 93:1601.
- Ogasa M, Naoko H, Murakami Y, Yoshikawa K (2013) Recovery performance in xylem hydraulic conductivity is correlated with cavitation resistance for temperate deciduous tree species. *Tree Physiol* 33: 335–344.
- Ogasa M, Utsumi Y, Miki N, Yazaki K, Fukuda K (2016) Cutting stems before relaxing xylem tension induces artefacts in *Vitis coignetiae*, as evidenced by magnetic resonance imaging. *Plant Cell Environ* 39: 329–337.
- Powell T, Galbraith D, Christoffersen B et al. (2013) Confronting model predictions of carbon fluxes with measurements of Amazon forests subjected to experimental drought. *New Phytol* 200: 350–365.
- Salleo S, Trifilò P, Esposito S, Nardini A, LoGullo MA (2009) Starch-to-sugar conversion in wood parenchyma of field-growing *Laurus nobilis* plants: a component of the signal pathway for embolism repair? *Funct Plant Biol* 36:815–825.
- Schreiber S, Hacke U, Hamann A, Thomas BR (2011) Genetic variation of hydraulic and wood anatomical traits in hybrid poplar and trembling aspen. *New Phytol* 190:150–160.
- Secchi F, Zwieniecki MA (2012) Analysis of xylem sap from functional (nonembolized) and nonfunctional (embolized) vessels of *Populus nigra*: chemistry of refilling. *Plant Physiol* 160:955.
- Secchi F, Pagliarani C, Zwieniecki MA (2017) The functional role of xylem parenchyma cells and aquaporins during recovery from severe water stress. *Plant Cell Environ* 40:858–871.
- Sperry J, Love DM (2015) What plant hydraulics can tell us about plant responses to climate-change droughts. *New Phytol* 207:14–27.
- Sperry J, Sullivan JEM (1992) Xylem embolism in response to freeze-thaw cycles and water stress in ring-porous, diffuse-porous, and conifer species. *Plant Physiol* 100:605–613.
- Sperry J, Perry A, Sullivan JEM (1991) Pit membrane degradation and air-embolism formation in ageing xylem vessels of *Populus tremuloides* Michx. *J Exp Bot* 42:1399–1406.
- Sperry JS, Venturas MD, Anderegg WRL, Mencuccini M, Mackay DS, Wang Y, Love DM (2017) Predicting stomatal responses to the environment from the optimization of photosynthetic gain and hydraulic cost. *Plant Cell Environ* 40:816–830.
- Torres-Ruiz JM, Sperry JS, Fernández JE (2012) Improving xylem hydraulic conductivity measurements by correcting the error caused by passive water uptake. *Physiol Plant* 146:129–135.
- Venturas M, MacKinnon E, Jacobsen A, Pratt RB (2015) Excising stem samples under native tens does induce xylem cavitation. *Plant Cell Environ* 38:1060–1068.
- Venturas MD, Sperry JS, Hacke UG (2017) Plant xylem hydraulics: what we understand, current research, and future challenges. *J Integr Plant Biol* 59:356–389.

- Wang Y, Pan R, Tyree MT (2015) Studies on the tempo of bubble formation in recently cavitated vessels: a model to predict the pressure of air bubbles. *Plant Physiol* 168:521.
- Wheeler J, Huggett B, Tofte A, Fulton R, Holbrook NM (2013) Cutting xylem under tension or supersaturated with gas can generate PLC and the appearance of rapid recovery from embolism. *Plant Cell Environ* 36:1938–1949.
- Wolf A, Anderegg WRL, Pacala SW (2016) Optimal stomatal behavior with competition for water and risk of hydraulic impairment. *Proc Natl Acad Sci USA* 113:E7222–E7230.
- Yang S, Tyree MT (1992) A theoretical model of hydraulic conductivity recovery from embolism with comparison to experimental data on *Acer saccharum*. *Plant Cell Environ* 15:633–643.